Pergamon

Bioorganic & Medicinal Chemistry, Vol. 3, No. 6, pp. 671–677, 1995

0968-0896/95 $9.50 + .00

0968-0896(95)00052-6

Perturbations in DNA Structure Upon Interaction with Porphyrins Revealed by Chemical Probes, DNA Footprinting and Molecular Modelling

Kevin G. Ford† and Stephen Neidle*

The CRC Biomolecular Structure Unit at The Institute of Cancer Research, Sutton, Surrey SM2 5NG, U.K.

Abstract—The interactions of several porphyrins with a 74 base-pair DNA sequence have been examined by footprinting and chemical protection methods. Tetra-(4-*N*-methyl-(pyridyl)) porphyrin (TMPy), two of its metal complexes and tetra-(4-trimethylanilinium) porphyrin (TMAP) bind to closely similar AT-rich sequences. The three TMPy ligands produce modest changes in DNA structure and base accessibility on binding, in contrast to the large-scale conformational changes observed with TMAP. Molecular modelling studies have been performed on TMPy and TMAP bound in the AT-rich minor groove of an oligonucleotide. These have shown that significant structural change is needed to accommodate the bulky trimethyl substituent groups of TMAP, in contrast to the facile minor groove fit of TMPy.

Introduction

It has been well established that a number of cationic porphyrin compounds with tetra *meso* substitution can bind to DNA. The best studied is *meso*-tetra-(4-*N*-methylpyridinium)porphyrin (TMPy) (Fig. 1a). This compound binds non-covalently to double-helical DNA,[1–5] with studies on synthetic polynucleotides showing that binding in GC regions is largely intercalative[4,6–9] whereas that in AT regions is external in nature, possibly involving the grooves of B-form DNA. Metal ions can be complexed to the porphyrin core, and their size and coordination number has a profound effect on the mode of DNA binding. Thus, tetradentate ion complexes of TMPy such as nickel (II) and copper (II)[10,11] behave in a very similar manner as the native TMPy, showing the same sequence-dependent binding modes, whereas complexes with hexadentate ions such as zinc (II), manganese[12,13] and cobalt[14] bind primarily to AT regions, in a non-intercalative manner.

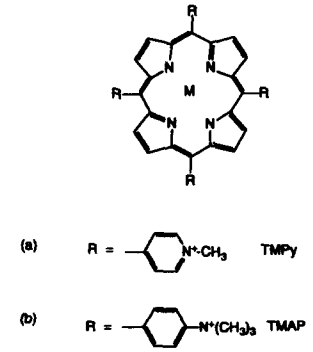

Figure 1. Chemical structures of DNA-binding porphyrins. M can be a metal ion.

†Present address: Department of Molecular Biology and Biotechnology, University of Sheffield, Sheffield S10 2UH, U.K.

The nickel–TMPy complex has been shown by footprinting methods to bind to both AT and GC regions,[15] with ligand-induced long-range conformational changes being apparent. This paper reports further footprinting data and examines the nature and extent of these changes by the use of specific chemical probes to DNA structure. We also report on the consequences of changing the *N*-methylpyridinium substituents of the porphyrin ring in TMPy to trimethylanilinium ones, in TMAP. Although X-ray crystallographic structures are not available for any porphyrin–DNA complexes, the available evidence does enable plausible structures to be postulated, with molecular modelling methods being used in the present study to provide molecular rationalisations for the footprinting and chemical probe findings.

Results

Footprinting

The results of DNA footprinting experiments on the four porphyrins with the MPE reagent, are shown in Figure 2, and the differential cleavage plots derived from the autoradiographs, are shown in Figures 3a–d. The metal-free porphyrin TMPy and its nickel complex have produced very similar cleavage patterns (Figs 3a,b) with inhibition of MPE cleavage at identical sites. However, there are marked differences in the relative degrees of protection. For TMPy itself, the most strongly protected sites are at nucleotides 28–30 (5'-TAT) and 35–37 (5'-ATA), with sites 23–25 (5'-AGC), 40–42 (5'-AAT) and 47–49 (5'-ATT) being more weakly protected. These last two are the most strongly protected from cleavage when the TMPy–Ni complex is used. The TMPy–Ni pattern shows a large enhancement

of cleavage at positions 37–39 (5'-AAA), which is only weakly seen in the metal-free porphyrin footprinting pattern. The same large enhancement of cleavage is seen with the TMPy–Pd complex (Fig. 3c); this has the major inhibition of cleavage at positions 28–30, with a majority of subsidiary sites being at or close to those for TMPy and TMPy–Ni. There is an additional strong site of protection at positions 17–19 (5'-TCC). The TMAP footprinting pattern (Fig. 3d) shows protection sites similar to those for the three TMPy compounds, with little evidence of enhanced cleavage.

Chemical probing

The patterns of diethylpyrocarbonate (DEPC) cleavage for the four compounds are shown in Figures 4a–d, with strong peaks corresponding to DEPC-reactive bases. The profiles are similar for all three TMPy compounds, e.g., those around positions 21–22 (5'-GG) and 34 (G). The patterns of reactivity for TMPy–Pd and TMPy–Ni in particular are closely similar in position (though not in relative intensities). The pattern of reactivity for TMAP (Fig. 4d), contrasts distinctly with the other porphyrins, with marked hyperreactivity occurring at positions 29 (A), 35–42 (5'-GATAAAAAT) and 47–48 (5'-AA).

The potassium permanganate cleavage plots are shown in Figures 5a–d. The extent of cleavage by $KMnO_4$ was observed to be significantly greater for reactions containing sample porphyrin than for DNA alone (Fig. 2c), suggesting porphyrin induced DNA conformational changes that increase the reactivity of this probe towards its target. The native TMPy compound shows (Fig. 5a) some modest hyperreactivity at a number of points in the sequence, primarily at positions 28–30 (5'-TAT), 42–44 (5'-TAT) and 48–50 (5'-ATT). There is a reduction in reactivity relative to the control at position 15 (T), which is seen in both other TMPy patterns (Figs 5b–c). These show hyperreactivity at position 16–17 (5'-TT), but little cleavage elsewhere along the sequence. The TMAP cleavage plot (Fig. 5d) shows significantly higher levels of reactivity than any of the TMPy ones, with pronounced hyperreactivity at positions 28–30 (5'-TAT) and 36–37 (5'-TA).

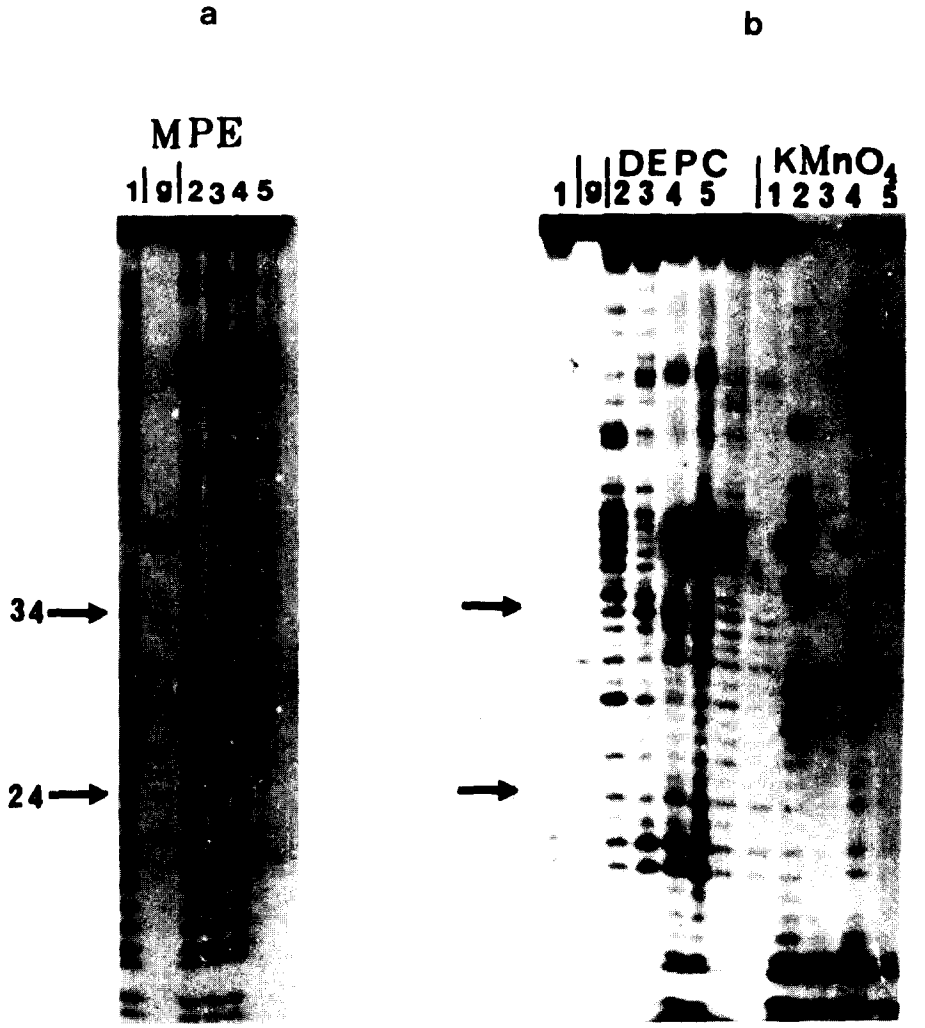

Figure 2. (a) MPE footprinting plots on the 74 base-pair DNA fragment. Lane 1 is a control, lane 2 is for TMAP, lane 3 is TMPy, lane 4 is TMPy–Ni and lane 5 is for TMPy–Pd, all at mM concentration and 10 min digestion. (b) DEPC and $KMnO_4$ reactivity patterns, for 15 min and 90 s reactivity times, respectively. In each case lane 1 is a control lane, lane 2 is TMAP, lane 3 is TMPy–Ni, lane 4 is TMPy and lane 5 is TMPy–Pd.

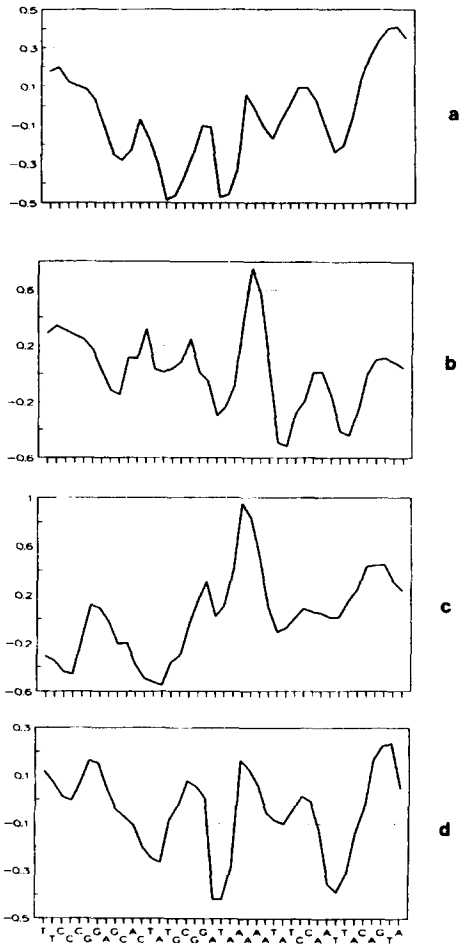

Figure 3. Fractional cleavage plots of the 74 base pair fragment derived from the MPE footprinting data for (a) TMPy, (b) TMPy–Ni, (c) TMPy–Pd, (d) TMAP.

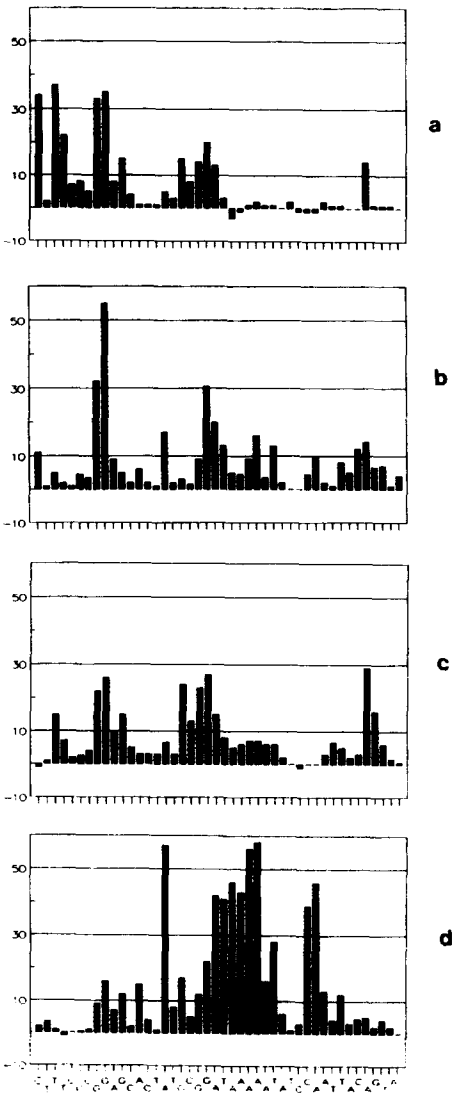

Figure 4. Bar histogram plots showing fractional cleavage of the 74 base pair fragment following DEPC treatment for (a) TMPy, (b) TMPy–Ni, (c) TMPy–Pd, (d) TMAP.

Molecular modelling

The TMPy molecule was fitted into the narrow minor groove of the d(CGCGAATTCGCG)$_2$ duplex with ease (Figs 6a,b). The mean plane of the porphyrin core is parallel to the phosphodiester backbones, and two adjacent *N*-methyl pyridine rings are buried in the groove, with the cationic nitrogen atoms *ca* 3.5–3.6 Å from thymine O2 atoms at the edges of AT base pairs. These *N*-methyl groups are in van der Waals contact with the atoms comprising the walls of the minor groove, and consequently little further movement of the DNA atoms took place during energy minimisation. The other two *N*-methyl groups of TMPy are directed away from the minor groove. The ligand binding site is 3–4 base pairs.

The TMAP molecule is distinguished from TMPy by its trimethylanilinium groups. When TMAP was located into the minor groove of the d(CGCGAATTCGCG)$_2$ duplex, visual inspection of the resulting structure (Figs 7a,b) showed that the molecule could be accommodated in a similar manner as TMPy, with two adjacent trimethyl groups being positioned deep into the minor groove, but accompanied by a large number of close intermolecular contacts between these methyl groups and the atoms forming the walls of the groove (mostly deoxyribose sugar atoms). The energy minimisation resulted in a stereochemically acceptable structure (Fig. 8), as a result of significant changes in the structure of the DNA. These changes are principally to minor-groove width (Fig. 9), with pronounced movements in phosphodiester backbone of up to 4 Å in the regions around the groove-bound trimethyl groups, producing two corresponding regions of wide minor groove. Small increases in major groove width were also apparent, as were perturbations to base pair geometry in terms of large propeller twist, buckle and roll angles at and around the site of TMAP binding. The minimised structure has both trimethylanilinium groups in proximity to the edges of some bases, with distances between O2 of thymine or N3 of adenine and the charged trimethylanilinium nitrogen atoms, of 3.8–4.2 Å, and a binding site size of *ca* four base pairs.

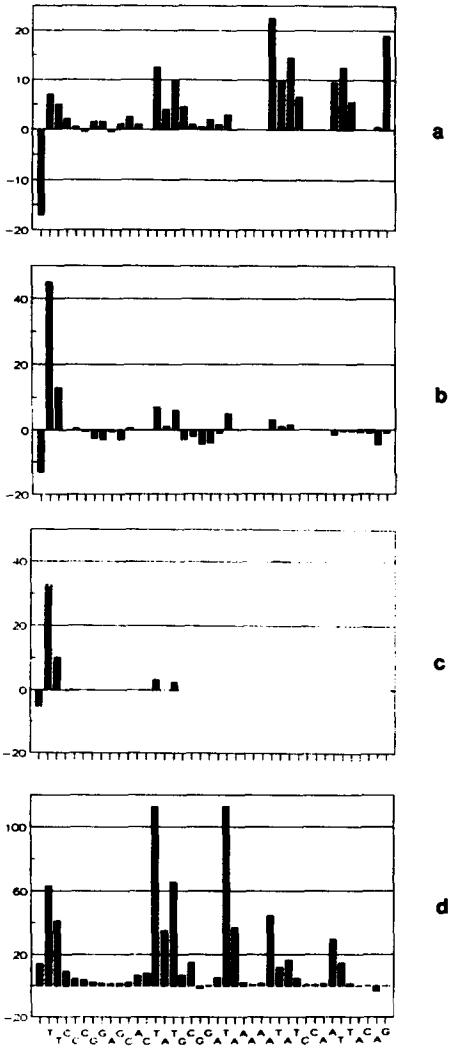

Figure 5. Bar histogram plots showing fractional cleavage following $KMnO_4$ treatment for (a) TMPy, (b) TMPy–Ni, (c) TMPy–Pd, (d) TMAP.

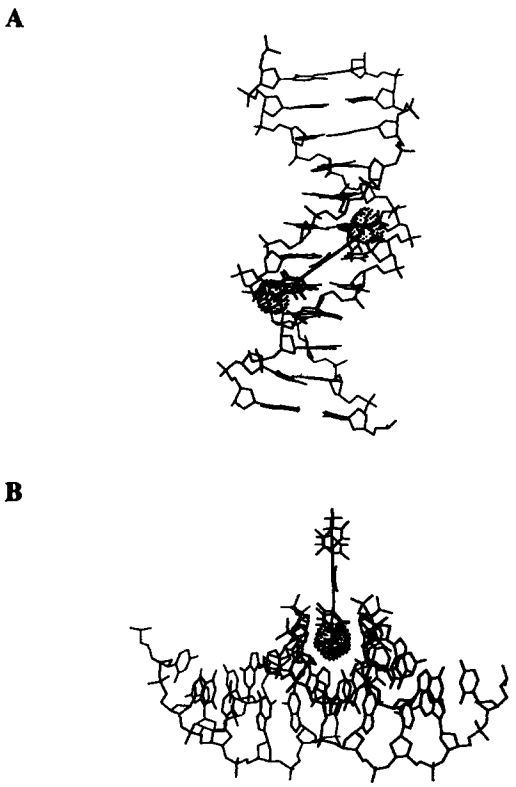

Figure 6. Two computer-generated views (drawn with the MIDAS program) of the molecular structure of the minor-groove complex between TMPy and the $d(CGCGAATTCGCG)_2$ duplex, with in each the van der Waals dot surface of the *N*-methyl groups of TMPy being shown (a) is with the helix axis of the DNA being vertical; (b) is a view along the minor groove, showing that the *N*-methyl groups of TMPy fit without excessive steric hindrance. The energy-minimised structures are very similar and are not shown here.

Discussion

The MPE footprinting studies, taken as a whole, indicate that the metal-free porphyrins TMPy and TMAP, as well as the nickel and palladium complexes of TMPy, have a strong preference for AT-containing sites. No sites inhibited from cleavage contain solely GC base pairs even though this 74 base pair sequence contains two such regions. Our previous footprinting study[15] on TMPy and TMPy–Ni used the enzyme DNase I as a footprinting agent. This did not reveal the same degree of preference for AT sites, since some GC sites were protected, especially when they contained the 5'-CpG step. Both footprinting studies concur in finding a majority of protected sites containing the 5'-TpA step. These distinct sequence preferences in the case of TMPy and its metal complexes that do not have axial ligands, have been previously rationalised by molecular-modelling studies[16,17] that have proposed intercalative binding at 5'-CpG steps and non-intercalative (possibly minor-groove) interactions at 5'-TpA sequences. Several biophysical methods summarised in Ref. 5, have shown that TMPy itself as well as its nickel, palladium and copper complexes, does bind intercalatively in GC regions. The footprinting technique is not able to define the mode of binding, although the differences in relative strengths of MPE cleavage inhibition (Figs 3a–c) suggest that this reagent is able to sense subtle differences between the DNA-binding behaviour of the three TMPy ligands that are not apparent with other techniques. The large enhancements to MPE cleavage in the extended A tract of the sequence that are only apparent with the two metal complexes, are also indicative of differences in ligand-induced DNA conformational change.

The MPE footprinting data presented here shows that TMAP has sequence-selective interactions with DNA, with preferences for AT-rich regions similar to the three TMPy ligands examined. This is in accord with earlier spectroscopic and viscometric studies[4–6] which also show that TMAP does not intercalate into any DNA sequences. Instead, it has been proposed that TMAP, uniquely for DNA-binding porphyrins, binds externally to the helix and self-stacks in some manner. There is no evidence of 10 base pair periodicity in our data, so a self-stacking model would not seem to be dictated by the helical repeat of the DNA.

A

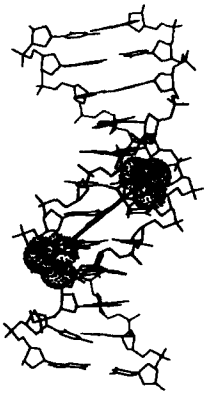

B

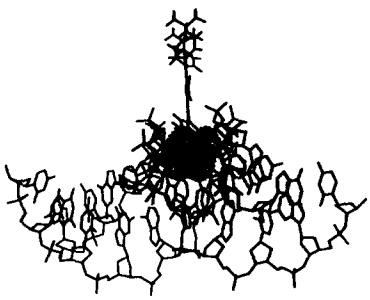

Figure 7. Two analogous views of the TMAP complex prior to energy minimisation. The trimethylanilinium groups are seen to be excessively large for fitting into the minor groove.

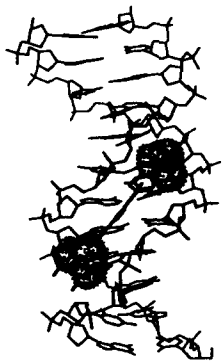

Figure 8. A view of the TMAP–d(CGCGAATTCGCG)2 complex after energy minimisation, showing that the trimethylanilinium groups are no longer in close contact with the walls and floor of the minor groove.

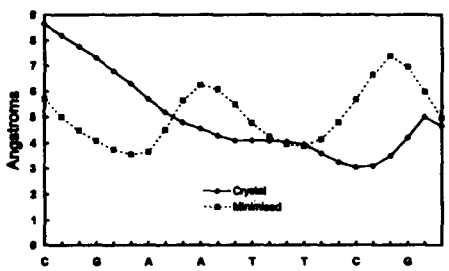

Figure 9. Plot of minor groove widths (in Å) for the crystallographic and energy-refined dodecanucleotide structures complexed to TMAP.

The two chemical probes used in this study are sensitive to changes in DNA conformation from the standard B-form structure for duplex DNA. DEPC reacts with the N7 atom of purines, which are normally only poorly accessible in a standard B-DNA structure. The potassium permanganate reagent reacts with the 5,6 bond of pyrimidines, especially thymine bases. Figures 4 and 5 together with the summary in Figure 10, show that each porphyrin induces some regions of probe accessibility in the 74 base pair DNA sequence. There are some differences between the metal-free TMPy porphyrin, and the two metal complexes, with the former showing less accessibility in the A tract of the sequence; this behaviour is paralleled by the enhanced MPE cleavage in this region of the DNA with TMPy–Ni and TMPy–Pd. We conclude that although all three TMPy ligands bind to the same sequences, there are real differences in their effects on neighbouring sequences. The nature of the metal ion coordinated with the porphyrin may impose differing conformational constraints on the porphyrin ring (such as the degree of induced pucker) that transmit to the local DNA sequence. The potassium permanganate sensitivity of thymines close to and within the TMPy binding sites (Fig. 5a) suggests that this ligand alone produces alterations in DNA structure that expose the 5,6 bond of these thymines.

The TMAP porphyrin produces changes in DNA structure that are quite distinct from those resulting from TMPy incubation. The very large DEPC reactivity in the A tract, at positions 34–42 (Fig. 5d) and in the TAT sequence (positions 28–30) are paralleled by high potassium permanganate reactivity in these regions. Both regions include TMAP binding sites, as indicated by MPE footprinting. The third strong TMAP binding site, at positions 47–51, shows mainly reactivity to DEPC. It is remarkable that these three TMAP sites are also TMPy binding sites; differences in chemical probe reactivity in these regions imply that TMAP and the TMPy ligands bind to the DNA sequences in distinct modes, or have differing effects on DNA structure. The non-intercalative (or partially intercalative) interactions at AT sites of the TMPy ligands produce relatively modest changes in DNA structure at and adjacent to the sites themselves, as predicted by previous molecular modelling studies.[16,17] The effects of TMAP, of producing alterations in DNA structure so as to render significant regions of DNA highly susceptible to chemical probes, are not obviously explained in terms of an external DNA-binding, self-stacking model;[5] binding to semi-melted regions of DNA has been suggested.[14] This issue is discussed further below.

The molecular modelling studies presented here provide evidence that the binding of TMPy and its metal complexes to DNA has similarities to the classic minor groove binders such as netropsin, berenil and pentamidine in that stereochemically plausible binding models can be constructed which have ligand bound in the AT-rich minor groove region of a B-DNA duplex, with minimal perturbation to B-DNA structure. This type of binding mode has been previously suggested[17] and is consistent with several lines of evidence; for example, linear dichroism measurements[14] have

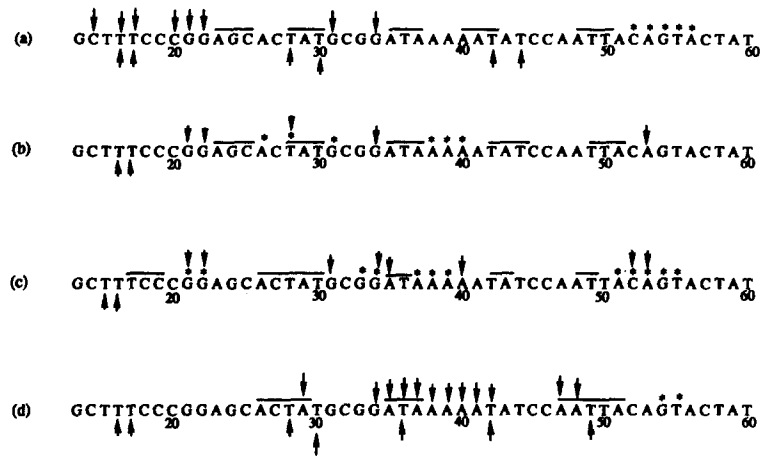

Figure 10. A summary of the footprinting and chemical protection data on the 74 base pair fragment. Ø = DEPC hyperreactivity, ≠ = $KMnO_4$ hyperreactivity, æ = MPE protected sites, * = MPE enhanced cleavage sites, for (a) TMPy, (b) TMPy–Ni, (c) TMPy–Pd, (d) TMAP.

demonstrated that the porphyrin plane in cobalt–TMPy is inclined to the DNA helix axis at an angle of *ca* 45°. Also the manganese–TMPy complex has been shown to cleave DNA by attack at the C1'-H1' bond, which is buried in the minor groove,[18] and is therefore consistent with minor groove binding. The model for TMPy–DNA minor groove binding presented here does not take account of any metal ions bound in the porphyrin ring. Their precise nature and their coordinated groups might be expected to perturb DNA structure to a greater extent than TMPy itself, although the chemical probe data (Figs 4 and 5) does not show any clear trend for the nickel and palladium complexes. Overall then, the TMPy–DNA minor groove binding model is structurally very similar to the crystal structures of oligonucleotide complexes with non-perturbing minor-groove ligands such as berenil and pentamidine.[19,20]

It has been possible in this study to produce a minor-groove binding model for the TMAP ligand. However by contrast with TMPy, it requires significant perturbations of the standard B-DNA structure in order for this to be achieved, on account of the size of the trimethylanilinium groups. Some of these changes are manifest in enlarged minor and major groove widths, which would result in enhanced susceptibility to chemical probes such as DEPC and $KMnO_4$. That these are indeed observed suggests that the perturbed minor-groove model is qualitatively consistent with the probe data, and that it may not be necessary to postulate other types of binding mode such as externally stacking around phosphate groups (which would not be likely to be sequence selective). In particular, the correspondence in AT-rich binding sites between the TMPy ligands and TMAP is strongly suggestive of a single type of sequence-selective interaction that exploits the particular steric and electronic features of AT minor grooves.

Experimental

Meso-tetra-(4-*N*-methylpyridyl)porphyrin (TMPy), as the metal-free tosyl salt, the nickel and palladium complexes as chloride salts, and the related *meso*-tetra-(4-trimethylanilinium)porphyrin (TMAP, Fig. 1b), were generously supplied by W. D. Wilson (Georgia State University). Stock solutions of them were prepared in 10 mM Tris buffer at pH 7.5, containing 10 mM NaCl.

Plasmid pBR322 (Sigma) was linearised with ECoRI and 3' end labelled with [a-^{32}P] dATP using Klenow enzyme (Pharmacia) according to published procedures.[21] The single-end labelled 74 base pair fragment used in these experiments was released by further digestion with ECoRV and Dde 1, and subsequently purified from an 18% polyacrylamide gel by diffuse elution from the excised gel slice. Following three rounds of phenol extraction to remove residual acrylamide, the labelled fragment was precipitated with ethanol, vacuum dried and taken up in 50 mL of 10 mM Tris (pH 7.4), 0.1 mM EDTA. Guanine specific markers (dimethyl sulphate–piperidine) were run in order to assign bands in the various digestion patterns.

Footprinting was performed with the MPE reagent methidium-propyl-EDTA (a gift from P. B. Dervan), according to published procedures.[22] Labelled DNA was incubated with porphyrin samples (25 mM final concentration) at room temperature for 15 min in 10 mM Tris (pH 7.8), 50 mM NaCl. DNA was recovered by rapid (–70 °C) ethanol precipitation. The products were analysed on 0.35 mM polyacrylamide gels containing 8M urea in TBE (0.1 M Tris, 0.9 M boric acid, 2.5 mM EDTA) buffer. Electrophoresis was typically at 1500 V for 2 h. Gels were dried onto Whatman 3 MM paper and subjected to autoradiography, overnight at –70 °C Autoradiograms were scanned with Joyce–Loebl and Molecular Dynamics densitomers. Data was processed to produce differential cleavage plots, representing ln ($F_L F_C$), where F_L and F_C are the fractions cleaved for each nucleotide step, for ligand (L) and control (C) respectively.

Chemical probe modifications were performed with diethylpyrocarbonate and potassium permanganate largely in accord with established procedures.[23,24] In the case of diethylpyrocarbonate, labelled DNA and DEPC

in 100 mM sodium cacodylate buffer (pH 7.2) and 10 mM EDTA was incubated with each porphyrin at room temperature for 15 min. Reaction was stopped by the addition of 1 M 2-mercaptoethanol in 1.5 M sodium acetate (pH 7.0). Potassium permanganate reactions were typically run for 60 s at room temperature, and were stopped in the same manner. Following ethanol precipitation, the resulting DNA pellet was resuspended in 1 M piperidine and heated to 90 °C for 15 min, followed by repeated further ethanol precipitation and lyophilization. The final DNA cleavage products were then run on DNA sequencing gels and the resulting autoradiograms processed as described above.

Molecular modelling studies were performed on Silicon Graphics Indigo and Pentium PC workstations. Molecular structures for TMPy and TMAP were constructed using the HYPERCHEM program (v4, Hypercube Inc.), and were energy-minimised using molecular mechanics with AMBER (v3) force-field parameters[25] together with additional values taken from the literature or derived by extrapolation. Atom-centred charges for TMPy and TMAP were obtained by MNDO semi-empirical calculations. These resulting structures were docked into the AT-region minor groove of the dodecanucleotide duplex structure of $d(CGCGAATTCGCG)_2$ with the aid of the MIDAS program,[26] using the crystallographic coordinates[27] for this structure taken from the Nucleic Acid Database.[28] Docked structures were considered to be stereochemically acceptable on the basis of having none or at most a small number of non-bonded contact distances less than the sum of atomic van der Waals radii. They were then subjected to molecular mechanics minimisations using the all-atom AMBER force-field for the DNA, a distance-dependent dielectric constant of $\varepsilon = 4r_i r_j/q_i q_j$[29] and a convergence criterion of completeness when shifts in successive minimisation cycles were less than 0.1 kcal mol^{-1} $Å^{-1}$.

Acknowledgements

This work was supported by the Cancer Research Campaign and the Science and Engineering Research Council/Celltech Ltd (CASE studentship to KGF).

References

1. Fiel, R. J.; Munson, B. R. *Nucleic Acids Res.* **1980**, *8*, 2835.

2. Pasternack, R. F.; Gibbs, E. J.; Villafranca, J. J. *Biochemistry* **1983**, *22*, 2406.

3. Pasternack, R. F.; Gibbs, E. J.; Villafranca, J. J. *Biochemistry* **1983**, *22*, 5409.

4. Carvlin, M. J.; Mark, E.; Fiel, R.; Howard, J. C. *Nucleic Acids Res.* **1983**, *11*, 6141.

5. Fiel, R. J. *J. Biomol. Struct. Dyn.* **1989**, *6*, 1259.

6. Banville, D. L.; Marzilli, L. G.; Strickland, J. A.; Wilson, W. D. *Biopolymers* **1986**, *25*, 1837.

7. Fiel, R. J.; Howard, J. C.; Mark, E. H.; Gupta, N. D. *Nucleic Acids Res.* **1979**, *6*, 3093.

8. Pasternack, R. F.; Garrity, P.; Ehrlich, B.; Davis, C. B.; Gibbs, E. J.; Orloff, G.; Giartosio, A.; Turano, C. *Nucleic Acids Res.* **1986**, *14*, 5919.

9. Marzilli, L. G.; Banville, D. L.; Zon, G.; Wilson, W. D. *J. Am. Chem. Soc.* **1986**, *108*, 4188.

10. Strickland, J. A.; Marzilli, L. G.; Wilson, W. D. *Biopolymers* **1990**, *29*, 1307.

11. Banville, D. L.; Marzilli, L. G.; Wilson, W. D. *Biochem. Biophys. Res. Commun.* **1983**, *113*, 148.

12. Bromley, S. D.; Ward, B. W.; Dabrowiak, J. C. *Nucleic Acids Res.* **1986**, *14*, 9133.

13. Ward, B.; Skorobogaty, A.; Dabrowiak, J. C. *Biochemistry* **1986**, *25*, 7827.

14. Sehlstedt, U.; Kim, S. K.; Carter, P.; Goodisman, J.; Vollano, J. F.; Norden, B.; Dabrowiak, J. C. *Biochemistry* **1994**, *33*, 417.

15. Ford, K.; Fox, K. R.; Neidle, S.; Waring, M. J. *Nucleic Acids Res.* **1987**, *15*, 2221.

16. Ford, K. G.; Pearl, L. H.; Neidle, S. *Nucleic Acids Res.* **1987**, *15*, 6553.

17. Hui, X.; Gresh, N.; Pullman, B. *Nucleic Acids Res.* **1990**, *18*, 1109.

18. Pitié, M.; Pratviel, G.; Bernadou, J.; Meunier, B. *Proc. Natl Acad. Sci. U.S.A.* **1992**, *84*, 3967.

19. Brown, D. G.; Sanderson, M. R.; Garman, E.; Neidle, S. *J. Mol. Biol.* **1992**, *226*, 481.

20. Edwards, K. J.; Jenkins, T. C.; Neidle, S. *Biochemistry* **1992**, *31*, 7104.

21. Sambrook, J.; Fritsch, E. F.; Maniatis, T. *Molecular Cloning: A Laboratory Manual*, 2nd ed., Cold Spring Harbor Laboratory Press; Cold Spring Harbour, New York, 1989.

22. van Dyke, M. W.; Hertzberg, R. P.; Dervan, P. B. *Proc. Natl Acad. Sci. U.S.A.* **1982**, *79*, 5470.

23. McLean, M. J.; Waring M. J. *J. Molec. Recognition* **1988**, *1*, 138.

24. McCarthy, J. G.; Williams, L. D.; Rich, A. *Biochemistry* **1990**, *29*, 6071.

25. Weiner, S. J.; Kollman, P. A.; Case, D. A.; Singh, U. C.; Ghio, C.; Alagona, G.; Profeta, S.; Weiner, P. *J. Am. Chem. Soc.* **1984**, *106*, 765.

26. Ferrin, T.; Huang, C. C.; Jarvis, L. E.; Langridge, R. *J. Mol. Graphics* **1988**, *6*, 13.

27. Dickerson, R. E.; Drew, H. R. *J. Mol. Biol.* **1981**, *149*, 7671.

28. Berman, H. M.; Olson, W. K.; Beveridge, D. L.; Westbrook, J., Gelbin, A.; Demeny, T.; Hsieh, S.-H.; Srinivasan, A. R.; Schneider, B. *Biophys. J.* **1992**, *63*, 751.

29. Orozco, M.; Laughton, C. A.; Herzyk, P.; Neidle, S. *J. Biomol. Struct. Dyn.* **1990**, *8*, 359.

(*Received in U.S.A.* 11 *October* 1994; *accepted* 6 *January* 1995)